STUDY ON FREQUENCY-DEPENDENT SITE AMPLIFICATION FACTORS FOR EARTHQUAKE EARLY WARNING SYSTEM

XIE Quancai [*] **Supervisor: Toshiaki YOKOI** [**]
MEE12601

ABSTRACT

In the current Earthquake Early Warning (EEW) systems, the site amplification factor is usually given as a scalar value empirically obtained. This study aims to study the method that estimates the frequency-dependent site amplification factors for EEW: one is site effects for B-Δ method, another is to design the casual recursive infinite impulse response (IIR) filter to model these factors and to simulate the spectra and accelerograms at target locations and also to evaluate the performance of IIR method.

First B-Δ relation is tested using 208 earthquakes recorded at IBH10 and IBRH19 of Kik-Net. The B-Δ relation obtained by curve fitting to the real data shows that the site condition does affect the relation. Second based on the idea of data assimilation, IIR filter method is tested using the same strong motion data: the surface ground motion at both sites are simulated from the corresponding borehole records using the IIR filter designed to fit the average spectral ratio of surface record to borehole's one; and the surface motion at IBRH10 is simulated from the surface records of IBRH19 using the IIR filter designed to fit the average spectral ratio of surface record of IBRH10 to that of IBRH19.The method using IIR filter shows a good performance in simulating acceleration waveforms and spectra for most of the event that I used and highly improve the accuracy of the seismic intensity estimation.

Keywords: B-Δ, Frequency dependent Site Amplification Factors, Casual Recursive IIR Filter.

1. INTRODUCTION

There are many papers which describe the science, engineering, and societal considerations of the active warning systems in the world. In the current Earthquake Early Warning (EEW) systems, the site amplification factor is usually given as a scalar value empirically obtained. I studied the frequency dependent site amplification factors in this paper. I got the data from the Kik-net (NIED) recorded at site IBRH10 and IBRH19 for 208 earthquakes. B-Δ relation is tested using 208 earthquakes recorded at IBH10 and IBRH19 of Kik-Net. I get the simulated results by using the IIR method for the same data.

2. RESULTS AND DISCUSSION

2.1. B- Δ method

[*]Institute of Engineering Mechanics (IEM), China Earthquake Administration (CEA), Harbin, China.
[**]Building Research Institute (BRI), Tsukuba, Japan.

By fitting Bt*exp (-At) function to the log-transformed acceleration waveform (UD component) envelope of the first two seconds or three seconds from the P onset, we extracted the envelope feature characteristics by 'A' and 'B' value. (Odaka et al., 2003; Kamigaichi, et al., 2004). I calculated the B value for the vertical component in the borehole (UD1) and on the ground surface (UD2) at IBRH10 and IBRH19. All the calculated results are shown in Figure 1 to Figure4. I calculated the B value from the P-wave onset time 2 seconds (Figure 1 and Figure 2) and 3 seconds (Figure 3 and Figure 4). The black curves in Figure 1 through Figure 4 show the currently used JMA formula: $\log_{10}B=-2.0008\log_{10}\Delta+3.9458$ where Δ is in km, B in gal/s (Noda et al., 2011). This formula is applied to all stations of the JMA EEW system, uniformly. The red curves in Figure 1,Figure 2,Figure 3,Figure 4 are those fitted to the data obtained from the borehole records, whereas the blue ones from the surface records. Comparison Figure 1 with Figure 2 and also comparison Figure 3 with Figure 4 show that there are not any significant differences among the fitted curves of the B values: one calculated using the time window 2 seconds and another 3 seconds. This is consistent with Odaka et al. (2003). In Figure 3 and Figure 4, the JMA B-Δ formula (black curves) are almost parallel to those estimated from the borehole and surface data in this station (red and blue ones, respectively) and are drawn above them. Especially to blue ones (surface records) the black curve shows a similarity.

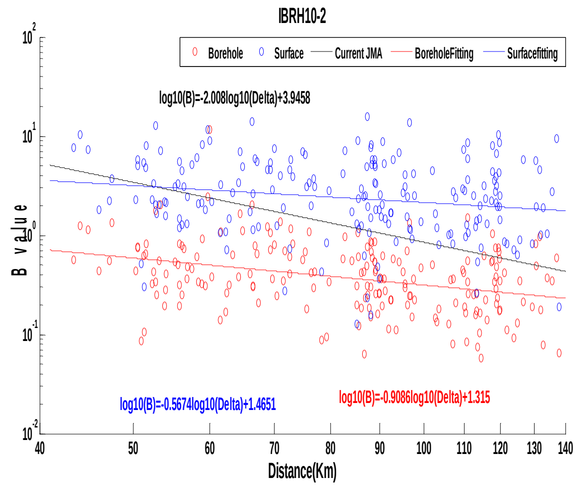

Figure 1. The B-Δ relationship at IBRH10 station: using 2 seconds after P wave arrival

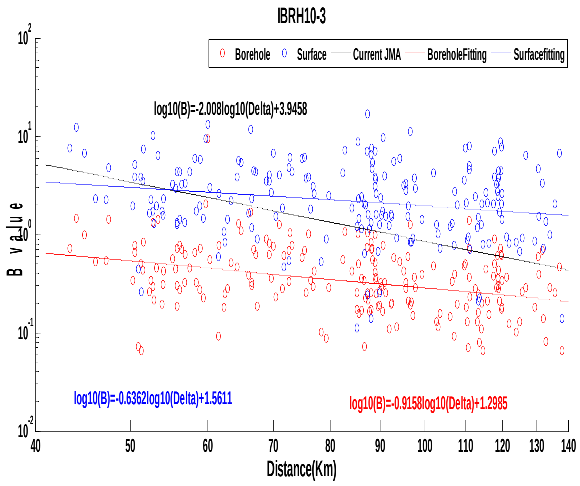

Figure 2. The B-Δ relationship at IBRH10 station: using 3 seconds after P wave arrival.

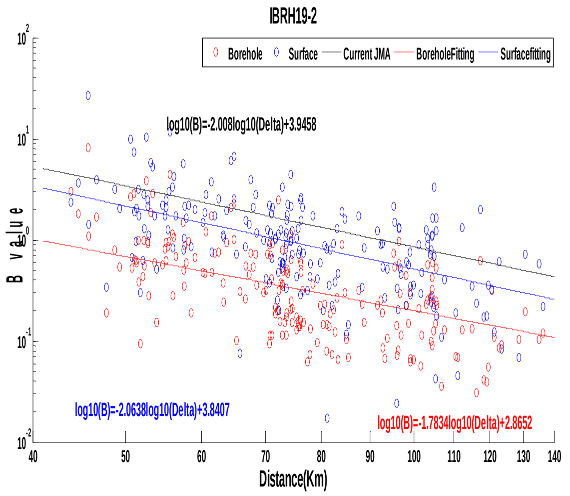

Figure 3. The B-Δ relationship at IBRH19 station: using 2 seconds after P wave arrival

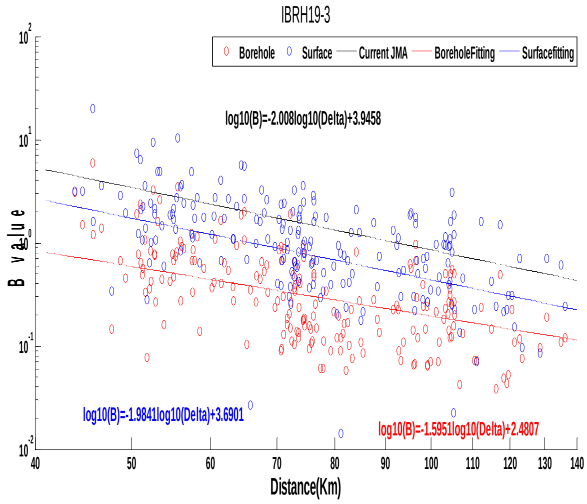

Figure 4. The B-Δ relationship at IBRH19 station: using 3 seconds after P wave arrival.

The formula fitted to the data of IBRH19 on the surface ($\log_{10}B=-2.0638\log_{10}\Delta+3.8407$ or $\log_{10}B=-1.9841\log_{10}\Delta+3.6901$) shows much similarity with the current JMA formula ($\log_{10}B=-2.0008\log_{10}\Delta+3.9458$). On other hands, in Figure 1 and Figure 2, this parallelism is lost. The black curves tend to stick to the blue one at short distance and to the red one at the long distance. The formula fitted by the data recorded by borehole sensor in IBRH10 ($\log_{10}B=-0.9068\log_{10}\Delta+1.3150$ or $\log_{10}B=-0.9158\log_{10}\Delta+1.2985$) shows much difference from the current JMA formula. Even in the same station, the blue curves calculated using the data recorded in the surface sensor are always drawn above the red curves calculated using the data recorded in the borehole sensor. This shows the site amplification factor did affect the B-Δ relationship as well as Nakamura et al. (2006) and JMA (2011) reported. It means that the parameter estimated in EEW systems is different when using the data obtained from different station or site condition even for the same earthquake. So for IBRH10, this difference cannot be ignored. We may use different B-Δ relationship according to different site conditions for more accurate calculation. More accurately, we may use the empirical B-Δrelation at each station for the correction of the B-Δ relationship for the EEW system. We may use the method proposed by Hoshiba (2013a and b) to skip the source estimate procedure as well in the future.

2.2. Simulation Between Two Stations

Next, we simulated waveforms at station IBRH10 using strong motion data recorded by the surface sensor at IBRH19. I show two examples of the 208 simulation results. The red curves are simulated results while the blues ones are observed results in Figure 5 through Figure 10. Figure 5 and Figure 6 show the simulation results for the M5.2 earthquake which occurred on Feb. 19, 2012. The amplification factors are about 4 (17.7→69.7 and 13.6→53.2) for horizontal component and about 4 (11.2→38.9) for vertical component. The increment of seismic intensity is 1.5(2.2→3.7). The seismic intensity difference between the observed surface acceleration and the simulated surface acceleration from the observed borehole acceleration is just 0.2 (3.5-3.7). When compared the observed acceleration and spectrum of the surface record with the simulated acceleration and spectrum, we can easily draw the conclusion that they are approximately simulated well. Figure 7 and Figure 8 show the simulation results for the M5.1 earthquake which occurred on April 14, 2011. The amplification factors are about 2 (7.0→16 and 7.0→17) for horizontal component and about 4 (4.2→16) for vertical component. The increment of seismic intensity is 1.4 (1.3→2.7). The seismic intensity residuals between the observed surface acceleration and the simulated surface acceleration from the observed borehole acceleration are 0.0 (2.7→2.7). When compared the observed acceleration and spectrum of the surface record with the simulated acceleration and spectrum, we can easily draw the conclusion that they are approximately simulated well. Compared these results during two earthquakes, the different amplifications of maximum acceleration reflect the differences of the frequent contents of the incident waveforms that cannot be reproduced by a scalar site amplification factor.

Although most of the simulation results show good performance of this method, some simulation results did not provide reasonable estimations. For example, Figure 9 and Figure 10 show the simulation results for the M5.3 earthquake which occurred on March 16, 2011. The amplification factors are about 6(6→34 and 5→36) for horizontal component and about 6 (3.8→22) for vertical component. The increment of seismic intensity is 2.3 (1.5→3.8). The seismic intensity difference between the observed surface acceleration and the simulated surface acceleration from the observed borehole acceleration is 1.1 (2.7→3.8). Comparison between observed and simulated accelerograms and spectra indicate that this simulation did not provide reasonable estimation. The observed amplification factors are about 2 (6→10 and 5→12) for horizontal component and about 1.5 (3.9→6.2) for vertical component.

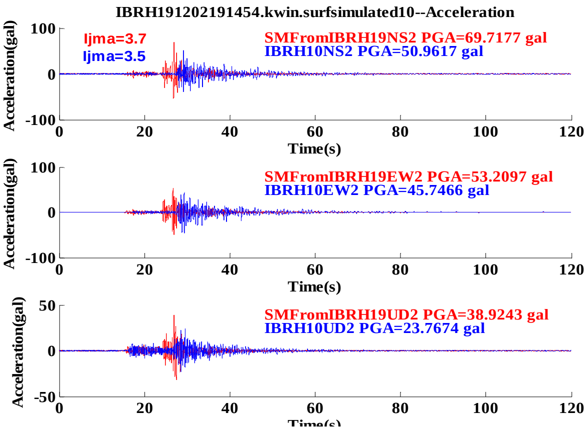

Figure 5. Comparison between the simulated and observed accelerograms for the earthquake 1202191454

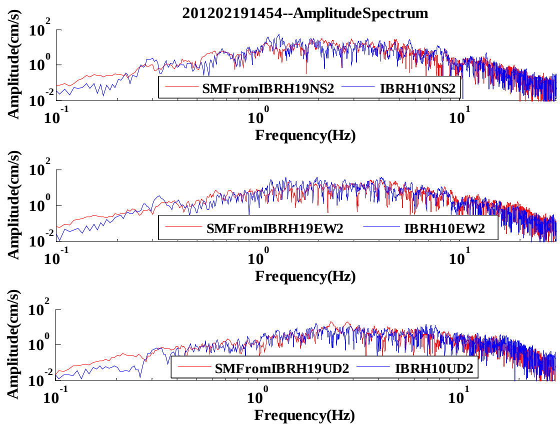

Figure 6. Comparison between the simulated and observed spectra for the earthquake 1202191454

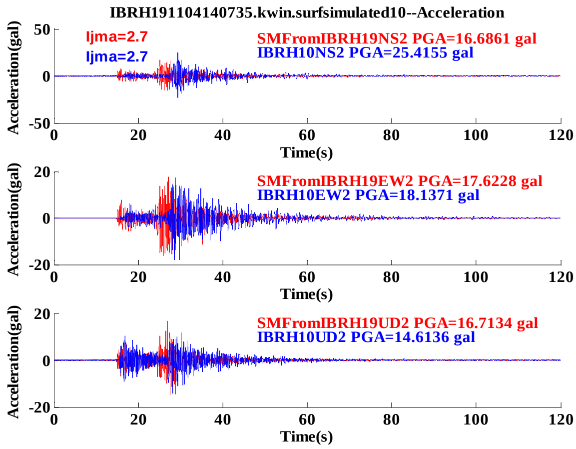

Figure 7. Comparison between the simulated and observed accelerograms for the earthquake 1104140735

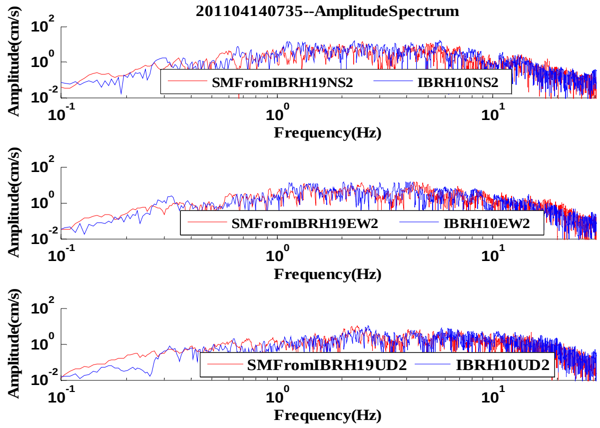

Figure 8. Comparison between the simulated and observed spectra for the earthquake 1104140735

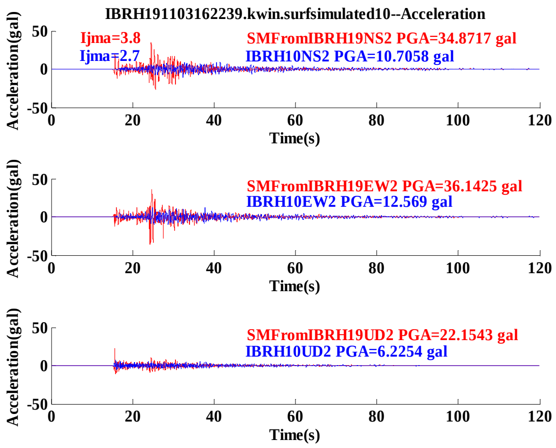

Figure 9. Comparison between the simulated and observed accelerograms for the earthquake 1103162239

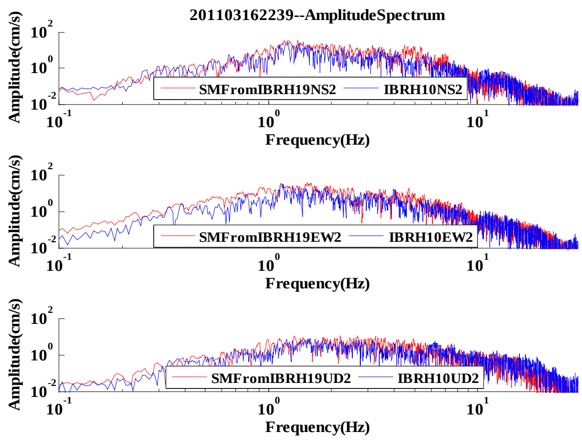

Figure 10. Comparison between the simulated and observed spectra for the earthquake 1103162239

I selected 40 earthquakes randomly from 208 earthquakes to calculate the observed seismic intensity and simulated one. The seismic intensity residuals are shown in Figure 11. The average seismic intensity difference of these 40 earthquakes is 0.31. The standard deviation of the residuals is 0.23. 67.5% of the difference is less than 0.3. 82.5% of the residuals are less than 0.5. 97.5% of the difference is less than 1. According to the paper (Iwakiri et al. 2011), JMA used ARV method based on topographic data, they investigated the station correction method based on empirical site amplifications obtained from recent observed seismic intensity data. Through the simple replacement of ARV by empirically estimated station corrections, they conclude that the number of residuals within+-1.0 was increased from 84% to 93%, and the number of the residuals within +-0.5 was increased from 55% to 59%. The comparison results between different methods are shown Table 1.

Table 1. The comparison result

Method	mean residual	standard deviation	+-0.5	+-1.0
ARV(Iwakiri et al. 2011),	0.25	0.63	55%	84%
Station Correction (Iwakiri et al. 2011),	0.19	0.55	59%	93%
Casual IIR Filter	0.31	0.23	82.5%	97.5%

Comparing with these results, we can conclude that the method used in this paper could improve the accuracy of the seismic intensity estimation and have good performance.

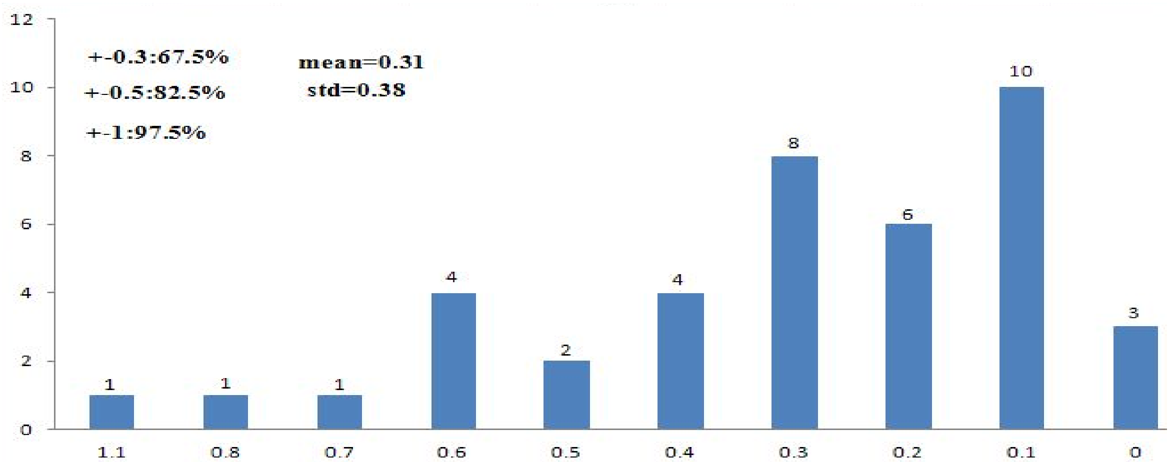

Figture 11. The residuals between the simulated seismic intensity and observed seismic intensity.

I evaluated the performance of this method using Kik-net data, the advantage of IIR method as shown below:

Comparison between the observed and simulated accelerograms and spectra indicate our method shows good performance for simulating acceleration and spectrum for most of the data used in this analysis. Compared the simulated results of different earthquakes, the different amplifications of maximum acceleration reflect the differences of the frequency content of the incident waveforms that cannot be reproduced by a scalar site amplification factor. This method highly improves the accuracy of the seismic intensity estimations in comparison with the current EEW systems. As the records of the front stations includes the real source factor and real wave propagation factor. The effects of rupture directivity, source extent and simultaneous multiple events are included in this method. An error of the source parameter estimate does not affect to the accuracy of the ground motion estimates by this method. It would have more excellent performance than current EEW systems, especially when considering some earthquakes which occurred simultaneously.

However, as shown in Figure 9 and Figure 10, the simulations did not provide reasonable estimations. The differences of site amplification factors are large. It may mean that the spectral ratio for this earthquake is not suitable. There exists the possibility that the IIR filter parameter may be sensitive to some effect not considered in this method. As the accuracy of this method depends on the filter design, we can characterize the IIR filter parameter by the iteration procedure more accurately mentioned in detail in Section 2.2. This problem may be overcome by more accurate design of the filter for these data. This method focused on the amplitude characteristics of site amplification factor and ignored the phase characteristics. When this method is applied to low frequency waves, phase characteristics may not be ignored. There had been very few researches on how to evaluate the phase information of site amplification factors. Although there were some researches, operation was performed in the frequency domain and then transformed to time domain, which is not suitable for EEW purpose. This difficulty may be improved by seismic interferometry using earthquake records triggered by small and intermediate size earthquake (e.g. Yamada et al., 2011) and more researches are needed to improve the accuracy of EEW systems.

3. CONCLUSIONS

The fitted B-Δ formulas for site IBRH10 and IBRH19 (Kik-net) were obtained using strong motion data recorded by the borehole and surface sensor. By the calculation, 12 spectral ratios were obtained. Using the casual recursive filter designed to fit the averaged spectral ratio and borehole records at IBRH10, I got 208 simulated surface accelerograms and spectra for IBRH10. Also, I got 208 simulated surface accelerograms and spectra for IBRH10 from surface records of IBRH19.

Our results suggest that the site condition does affect the B-Δ relationship. I suggested some solutions that can improve the current B-Δ Method. We can use different B-Δ relationship according to different site conditions for more accurate calculation. More accurately, we may use the empirical B-Δ relation at each station for the correction of the B-Delta relationship for the EEW system. We may also use the IIR method proposed by Hoshiba (2013a and b) to skip the source parameter estimate procedure. IIR method has good performance in simulating acceleration and spectra for most of the data used in my analysis and highly improve the accuracy of the seismic intensity estimation when compared with the current EEW systems. The accuracy of IIR Filter method depends on the accuracy of the input spectral ratio and the design of the IIR filter. A possibility for accuracy improvement by using larger number of first order and second order filter, however, the design procedure of this filter will be time consuming. I have made an action plan to do some research and education about the EEW in China.

ACKNOWLEDGEMENTS

I would like to express my heartiest gratitude to Dr. Mitsuyuki Hoshiba (MRI/JMA) for supervising me and giving me very useful advices and suggestions during my individual study. Thanks to NIED for providing the strong motion data. The JMA Seismic Intensity is calculated by ViewWave developed by Dr. Toshihide Kashima.

REFERENCES

Hoshiba, M., 2013a, J. Geophys. Res.: Solid Earth, 118, 1–13.
Hoshiba, M., 2013b, in press.
Iwakiri,K., et al.., 2011, Earth, Planets and Space.63, 57-69.
Japan Meteorological Agency, 2011, JMA Report, in Japanese.
Kamigaichi, O., et al., 2009, Seism. Res. Lett., 80, 717–726.
Nakamura, H., et al., 2009, Geophys. Res. Lett., 36.
Noda, S., et al., 2011, RTRI REPORT Vol. 25, No. 7, Jul. (in Japanese with English Abstract).
Odaka, T., et al., 2003, Bill. Seism. Soc. Am., 93, 526–532.
Yamada,M., et al. 2010, J. Geophys. Res., 115, B03302.